Nonlinear Phenomena in Bromate-Bromide-Cerium(III) System in a Continuous-Flow Stirred Tank Reactor: Reaction Behavior near the Crossing Point in a Cross-Shaped Phase Diagram

Yoshihiro SASAKI
Institute for Chemical Research, Kyoto University, Uji, Kyoto 611
(Received December 2, 1989)

The behavior of a bromate-bromide-cerium(III) system in a continuous-flow stirred tank reactor was simulated near the crossing point in the cross-shaped phase diagram obtained by using linearized stability analysis. The transitions between monostable states and an oscillatory state occur through supercritical and subcritical Hopf bifurcations. The steady states (SSI and SSII) in the neighborhood of the bifurcation points of the subcritical Hopf bifurcations are excitable against perturbations of the concentration of bromide. Some properties of the excitation were also examined. Complicated bifurcations associated with excitability are found in the bistable region near the crossing point. In order to understand bistability and oscillations in this system, the dynamical behavior of a five-variable model was examined by means of a two-variable approximation.

The bromate-bromide-cerium(III) system in a sulfuric acid medium in a continuous-flow stirred tank reactor (CSTR) can possess either one or two steady states, or even an oscillatory state.[1-4] The reaction behavior of the system has been successfully reproduced through the FKN reaction mechanism.[2,4-6] Field and Försterling prepared a new set of the rate constants of the mechanism (FF set) on the basis of recent kinetic studies.[7] A simulation using the FF set of rate constants also coincided with the experiments; the application of linearized stability analysis to this system brought a cross-shaped phase diagram, resembling that found in a rather simple model proposed by Boissonade and De Kepper.[8-10] The model exhibits a complex bifurcation profile near the crossing point of the phase diagram, based on the nonlinearity of the model.[9,11] While analytical studies for real chemical reaction systems are very difficult, it is important to confirm the existence of such complicated bifurcations in them. This paper describes the behavior of a bromate-bromide-cerium(III) system in a CSTR near the crossing point of a cross-shaped phase diagram.

Calculations

The FKN scheme of the bromate-bromide-cerium(III) system can be represented as follows:

$$Br^- + HOBr + H^+ \rightleftarrows Br_2 + H_2O \quad (1)$$

$$Br^- + HBrO_2 + H^+ \longrightarrow 2HOBr \quad (2)$$

$$Br^- + BrO_3^- + 2H^+ \rightleftarrows HOBr + HBrO_2 \quad (3)$$

$$2HBrO_2 \longrightarrow HOBr + BrO_3^- + H^+ \quad (4)$$

$$HBrO_2 + BrO_3^- + H^+ \rightleftarrows 2BrO_2\cdot + H_2O \quad (5)$$

$$Ce(III) + BrO_2\cdot + H^+ \rightleftarrows Ce(IV) + HBrO_2 \quad (6)$$

In this calculation, we used the FKN mechanism and the FF set of the rate constants (Table 1).[7] Because the reaction system was studied in a CSTR, the terms $k_0(C_{0i}-C_i)$ were added to the rate equations generated from Reactions 1—6, where C_i and C_{0i} are the concentrations of species i in the solution and in the feed flow, respectively, and k_0 is the reciprocal of the residence time. The external parameters for the system in a CSTR are $[BrO_3^-]_0$, $[Br^-]_0$, $[Ce(III)]_0$, $[H^+]_0$, k_0, and the temperature. In this simulation, the values of $[H^+]_0$, $[Ce(III)]_0$, k, and temperature were fixed and seven-variable equations were employed, since the value of $[H^+]_0$ was very large.

Table 1. FF Set of Rate Constants at 20 °C

Reaction	Forward	Backward
1	8×10^9 $M^{-2}s^{-1}$	110 s^{-1}
2	3×10^6 $M^{-2}s^{-1}$	—
3	2 $M^{-3}s^{-1}$	3.2 $M^{-1}s^{-1}$
4	3000 $M^{-1}s^{-1}$	—
5	42 $M^{-2}s^{-1}$	4.2×10^7 $M^{-1}s^{-1}$
6	8×10^4 $M^{-2}s^{-1}$	8.9×10^3 $M^{-1}s^{-1}$

1M=1 mol dm^{-3}.

Calculations of the steady states were performed by Newton's method. The stability of the steady states was analyzed by means of a linearized stability analysis. The temporal evolution of the system was calculated by using Gear's method.[12]

Results and Discussion

The application of linearized stability analysis to the bromate-bromide-cerium(III) system in a CSTR shows that the system exists in either of four states when $[H^+]_0$=0.75 M (1 M=1 mol dm^{-3}), $[Ce(III)]_0$=3×10^{-4} M, and k_0=0.005 s^{-1}, as shown in Fig. 1. The four states are SSI (a high concentration of Br^- and a low concentration of Ce(IV)), SSII (a low concentration of Br^- and a high concentration of Ce(IV)), a bistable state, and an oscillatory state. The system in region d possesses two unstable nodes (foci) and one saddle point; it evolutes temporally along a stable limit cycle. The system in region e possesses one unstable node (focus), one saddle point, and one stable node (focus); it then settles down in the stable node

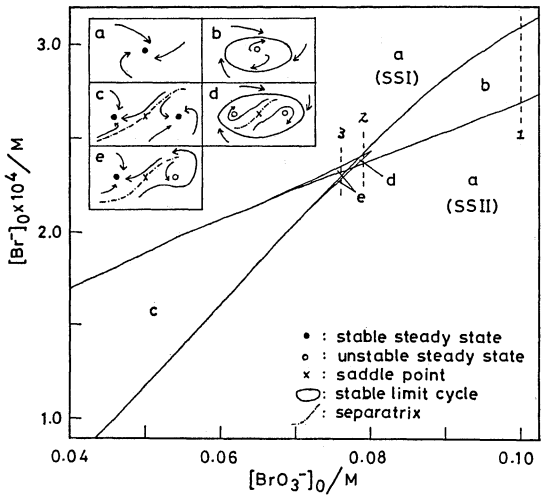

Fig. 1. Phase diagram in the $[BrO_3^-]_0$-$[Br^-]_0$ subspace, obtained by using linearized stability analysis and phase portraits. $[H^+]_0$=0.75 M, $[Ce(III)]_0$=3×10^{-4} M, and k_0=0.005 s^{-1}.[1)]
a: monostable region (SSI or SSII), b: oscillatory region, c: bistable region, d: region having three unstable steady solutions, e: region having one stable and two unstable steady solutions. 1: $[BrO_3^-]_0$ =0.1 M, 2: $[BrO_3^-]_0$=0.079 M, 3: $[BrO_3^-]_0$=0.076 M.
1) The values of the external parameters are applicable to Figs. 2—6.

(focus).[13)] Cross-shaped phase diagrams similar to that shown in Fig. 1 were observed in a bromate-bromide-manganese(II) system in a CSTR as well as in many nonlinear reaction systems.[10,14)]

Figures 2 and 3 show the dependency of the amplitude and period in the oscillations of the system on the concentration of Br^- in the feed flow when $[BrO_3^-]_0$ =0.1 and 0.079 M, respectively. The sign of Re(λ) (λ: eigen value) obtained by means of the linearized stability analysis changes at the dashed lines in the figures. When $[BrO_3^-]_0$=0.1 M (1 in Fig. 1), the amplitude of the oscillations varies remarkably near SSI and SSII. On the other hand, when $[BrO_3^-]_0$ =0.079 M (2 in Fig. 1), the amplitude of the oscillations is approximately constant over all the oscillatory region, and hysteresis can be found near SSI and SSII. Though the period of the oscillations trends to increase in magnitude near SSI and SSII, its value does not approach infinity at the end of the oscillatory region. The bifurcation in Fig. 2 is consistent with the supercritical Hopf bifurcation, and the bifurcation in Fig. 3 is equal to the subcritical Hopf bifurcation.[15)] Our result that the subcritical Hopf bifurcation is induced in a relatively neighboring region to the crossing point in Fig. 1 is consistent with that obtained by Boissonade and De Kepper.[9)] The existence of a supercritical Hopf bifurcation is experimentally confirmed in the bromate-bromide-manganese(II) system in the CSTR mode.[14)] It may be difficult to confirm the existence of subcritical Hopf bifurcation in the bromate-bromide-cerium(III) system

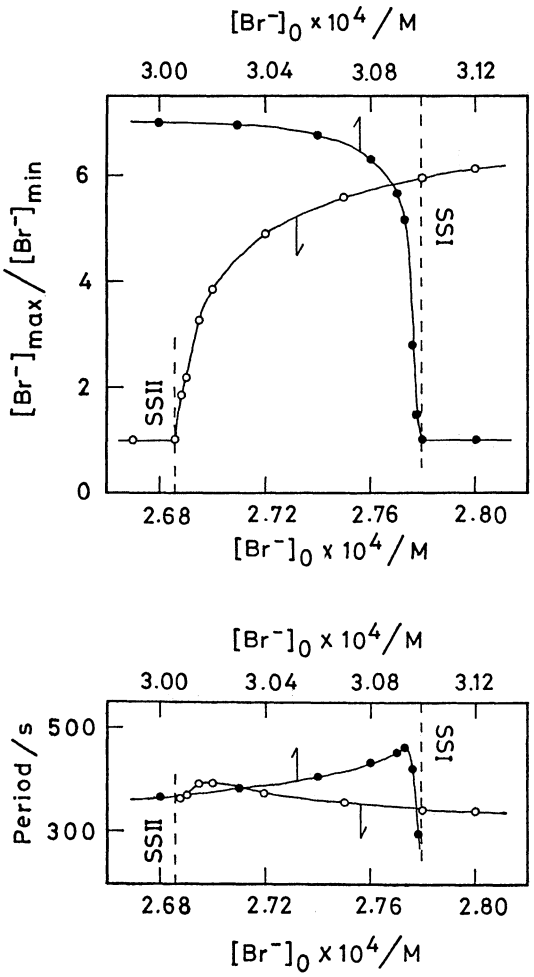

Fig. 2. Amplitude and period of the sustained oscillations when $[BrO_3^-]_0$=0.1 M.
The sign of Re(λ) (λ: eigen value) changes at the dashed lines.

experimentally because the range of $[Br^-]_0$ exhibiting hysteresis is very narrow. Gáspár et al. found that there are some points where an oscillatory state and a monostable state co-exist near the borders of an oscillatory region in the bromate-bromide-ferroin system.[16)] This may result from a subcritical Hopf bifurcation.

Figure 4 shows the excitability of some steady states near the dashed lines in Figs. 2 and 3, induced by sudden changes in the bromide concentration at time zero.[17)] The steady states can be perturbed by adding Br^- or Ag^+ ions to the system.[18)]

When $[BrO_3^-]_0$=0.1 M, the system in SSII is not excitable against a sudden increase of the bromide concentration. On the other hand, the system in SSI exhibits a major excursion, depending on the magnitude of the decrease of the bromide concentration, followed by damped oscillations (Fig. 4a). Though the response when $[Br^-]=4.5\times10^{-7}$ M at time zero is different from that when $[Br^-]=6.5\times10^{-7}$ M at time zero, the response depends on the magnitude of the continuous perturbation in the bromide concen-

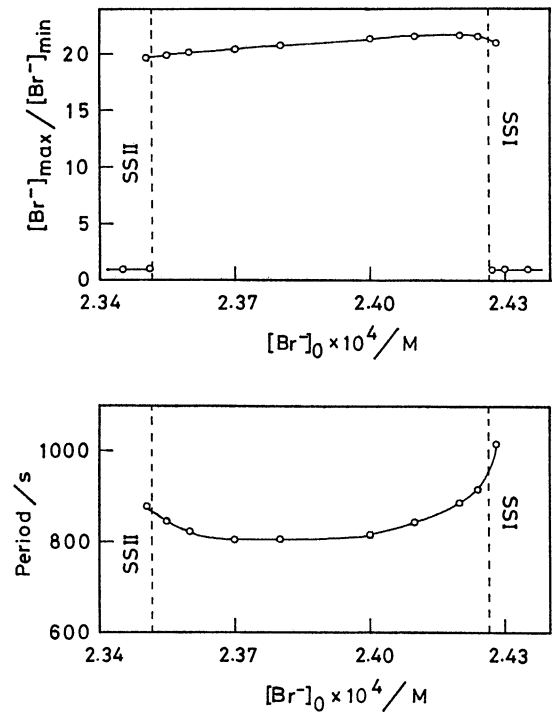

Fig. 3. Amplitude and period of the sustained oscillations when $[BrO_3^-]_0$=0.079 M.
The sign of Re(λ) (λ: eigen value) changes at the dashed lines.

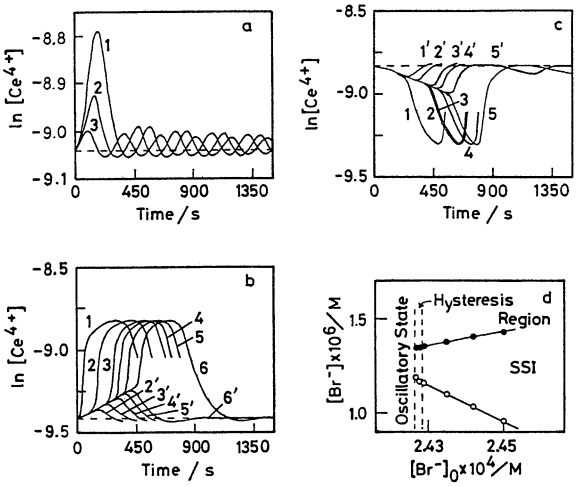

Fig. 4. Excitability of the steady states (SSI and SSII) when $[BrO_3^-]_0$=0.1 and 0.079 M.
a: $[BrO_3^-]_0$=0.1 M, $[Br^-]_0$=3.1×10^{-4} M, $[Br^-]_{ss}$=1.19675×10^{-6} M, and 10^7[Br$^-$]/M=4.5 (1), 5.5 (2), and 6.5 (3). b: $[BrO_3^-]_0$=0.079 M, $[Br^-]_0$=2.435×10^{-4} M, $[Br^-]_{ss}$=1.37610×10^{-6} M, and 10^6[Br$^-$]/M=0.5 (1), 1.09 (2), 1.10 (2′), 1.0972 (3), 1.0973 (3′), 1.097225 (4), 1.097226 (4′), 1.09722572 (5), 1.09722573 (5′), 1.0972257262 (6), and 1.0972257263 (6′). c: $[BrO_3^-]_0$=0.079 M, $[Br^-]_0$=2.345×10^{-4} M, $[Br^-]_{ss}$=3.18913×10^{-7} M, and 10^6[Br$^-$]/M=1.43 (1′). 1.44 (1), 1.4326 (2′), 1.4327 (2), 1.432698 (3′), 1.432699 (3), 1.43269825 (4′), 1.43269826 (4), 1.4326982578 (5′), and 1.4326982579 (5). d: dependency of the threshold value in SSI on $[Br^-]_0$ when $[BrO_3^-]_0$=0.079 M (○: threshold and ●: stable steady state).

tration.

When $[BrO_3^-]_0$=0.079 M, the system responds to the perturbation in the bromide concentration in another way, as shown in Figs. 4b and 4c. These figures suggest that there are thresholds with regard to the bromide concentration. When the bromide concentration at time zero is near the thresholds, the system responds very sensitively to even a slight difference in the [Br$^-$] value. When the bromide concentration at time zero is within the thresholds, the system settles down in the primary steady states with damped oscillations. However, such a perturbation, in which the bromide concentration exceeds the thresholds, induces the system to start a major excursion. The maximum concentration of Ce(IV) in the excursion is constant and the induction period after which the excursion occurs depends on the strength of the perturbation. As shown in Fig. 4d, the separation between the threshold in SSI and the $[Br^-]_{ss}$ value of SSI decreases along with a decrease of $[Br^-]_0$; the threshold is smoothly jointed to the threshold of the subcritical Hopf bifurcation.[19]

Figure 5 shows some properties of the excitation of the system in SSI when $[BrO_3^-]_0$=0.079 M and $[Br^-]_0$ =2.435×10^{-4} M. If the concentration of bromide is perturbed from the $[Br^-]_{ss}$ value of SSI (1.37610×10^{-6} M) to 1.25×10^{-6} M at time zero, the system exhibits no excitation (1 in Figs. 5a and 5b). The value of [Br$^-$] then varies rapidly toward the steady-state value. When the system is stimulated with the same perturbation five times at intervals of 10^{-4} s, as shown in Fig.

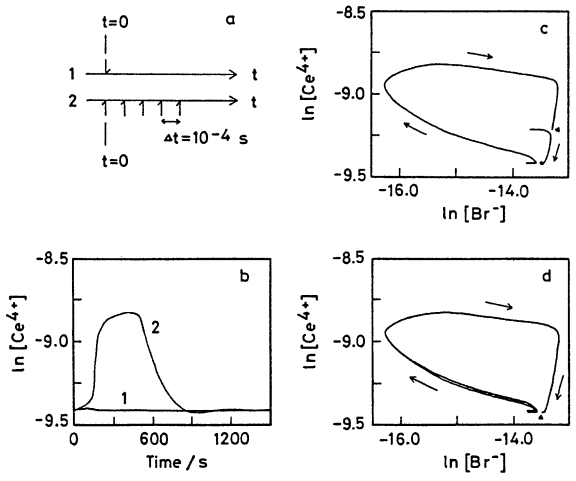

Fig. 5. Properties of excitation of the steady state (SSI) when $[BrO_3^-]_0$=0.079 M and $[Br^-]_0$=2.435×10^{-4} M.
1 in a and b: perturbed from the $[Br^-]_{ss}$ value (1.37610×10^{-6} M) to 1.25×10^{-6} M at time zero. 2 in a and b: perturbed from the $[Br^-]_{ss}$ value to 1.25×10^{-6} M five times at intervals of 10^{-4} s. In c and d, [Br$^-$] is perturbed from the $[Br^-]_{ss}$ value to 1.05×10^{-6} M at time zero. c and d: perturbed by the same manner again at 600 s (at the point indicated by the mark (▲) in Fig. 5c) and at 900 s (at the point indicated by the mark (▲) in Fig. 5d) respectively.

5a (notation 2), it exhibits a major excursion (Fig. 5b (notation 2)). This suggests that the system in SSI also gets excited when the concentration of bromide is perturbed weakly for a long time. A similar excitability is observed in a bromate-cerium-oxalic acid system.[20,21] When the concentration of bromide is perturbed from the $[Br^-]_{ss}$ value of SSI to 1.05×10^{-6} M at time zero, the system becomes excited. The $[Br^-]$ value overshoots its steady-state value at *ca.* 400 s and slowly decays to its steady state value. The [Ce(IV)] value starts a major excursion at *ca.* 80 s and begins damped oscillations at *ca.* 900 s. Figures 5c and 5d show the behavior of the system when the system being excited by the perturbation described above at time zero is stimulated again by the same perturbation at 600 and 900 s, respectively. When the system is stimulated at 600 s, the value of $[Br^-]$ is restored rapidly to its former value and the system does not become excited again. On the other hand, when the system is stimulated at 900 s, the system becomes excited. The property of excitation shown in Figs. 4 and 5 is consistent with that of an excitation in a nervous system.

The linearized stability analysis for the bromate-bromide-cerium(III) system in a CSTR shows that the system possesses two stable foci in the $[Br^-]_0$ range of 2.3023×10^{-4}—2.3051×10^{-4} M when $[BrO_3^-]_0=0.076$ M (3 in Fig. 1). We simulated the dependency of the behavior of the bistable system on the change of $[Br^-]$ value from the $[Br^-]_{ss}$ value. Figures 6a and 6b show the behaviors of the system when $[Br^-]_0=2.304\times10^{-4}$ M. The system in SSII returns to the steady state with damped oscillations when the bromide concentration is perturbed from the $[Br^-]_{ss}$ value of SSII (3.15949×10^{-7} M) to 9.2×10^{-7} M. However, the system suddenly goes to SSI at *ca.* 2700 s when the bromide concentration is perturbed to 9.9×10^{-7} M. On the other hand, the system in SSI returns to the primary steady state via a major excursion by the decrease of the bromide concentration from the $[Br^-]_{ss}$ value of SSI (1.34974×10^{-6} M) to 1.1852×10^{-6} M. Figures 6c and 6d show the behaviors of the system induced by sudden changes of the bromide concentration when $[Br^-]_0=2.303\times10^{-4}$ M. The figures suggest that there are thresholds in regard to the bromide concentration and that if the bromide concentration exceeds the thresholds by the perturbation the system in SSI or SSII transfers to an oscillatory state.

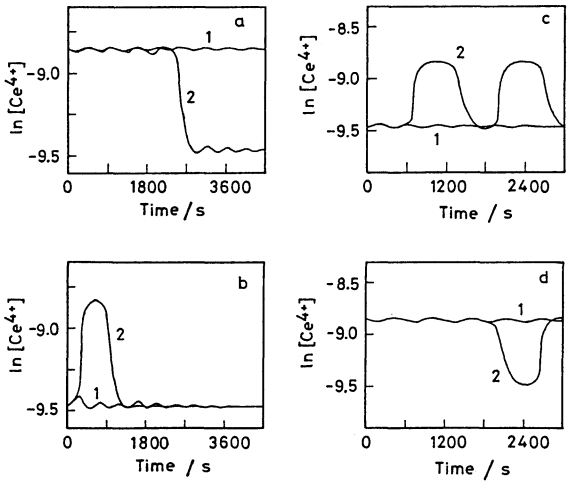

Fig. 6. Behaviors of the bistable system induced by sudden changes of $[Br^-]$ at time zero when $[BrO_3^-]_0=0.076$ M.
a: $[Br^-]_0=2.304\times10^{-4}$ M, $[Br^-]_{ss}=3.15949\times10^{-7}$ M (SSII), and $[Br^-]=9.2\times10^{-7}$ M (1) and 9.9×10^{-7} M (2). b: $[Br^-]_0=2.304\times10^{-4}$ M, $[Br^-]_{ss}=1.34974\times10^{-6}$ M (SSI), and $[Br^-]=1.1853\times10^{-6}$ M (1) and 1.1852×10^{-6} M (2). c: $[Br^-]_0=2.303\times10^{-4}$ M, $[Br^-]_{ss}=1.34504\times10^{-6}$ M (SSI), and $[Br^-]=1.21\times10^{-6}$ M (1) and 1.20×10^{-6} M (2). d: $[Br^-]_0=2.303\times10^{-4}$ M, $[Br^-]_{ss}=3.14161\times10^{-7}$ M (SSII), and $[Br^-]=1.09\times10^{-6}$ M (1) and 1.10×10^{-6} M.

Our simulation shows that supercritical and subcritical Hopf bifurcations take place in the bromate-bromide-cerium(III) system and that the steady state of the system is excitable near the hysteresis ranges of the subcritical Hopf bifurcations as well as in region e of Fig. 1 and in the bistable region near the crossing point in the cross-shaped phase diagram, as described below. The result, that the steady state of the system is excitable near the bifurcation point for a subcritical Hopf bifurcation, resembles the experiment and the calculation for Belousov-Zhabotinsky (BZ) reaction system.[18,22,23] It is not easy to explain why a steady state near the bifurcation point for a subcritical Hopf bifurcation is excitable. The types of the bifurcations described above are depicted in Figs. 7a and 7b, where μ represents a bifurcation parameter and μ_c a critical point of μ. In this study, $[Br^-]_0$ corresponds

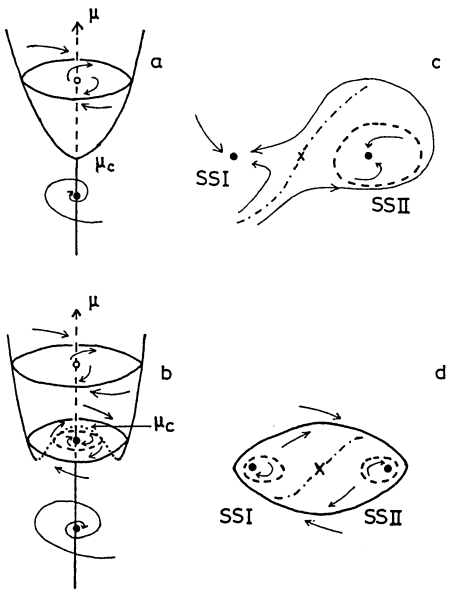

Fig. 7. Hopf bifurcations and phase portraits.
a: supercritical Hopf bifurcation, b: subcritical Hopf bifurcation, c: phase portrait for Figs. 6a and 6b, d: phase portrait for Figs. 6c and 6d.

to μ. In a subcritical Hopf bifurcation, an unstable limit cycle appears in the hysteresis range of μ existing near the critical point. The stable and the unstable limit cycles couple together and disappear at the end of the hysteresis range and only the globally attracting stable focus remains. Under the reaction conditions described in Figs. 4b and 4c, there is a globally attracting stable focus in the phase space of this reaction system. However, it may be possible that a quasilimit-orbit zone is left behind the disappearence of the stable and the unstable limit cycles and we presume that the width of the zone is very narrow and that a state of this system, existing in the outside of the zone at time zero, moves temporally around the zone and then goes to the stable focus.[24] If we assume that this is true, we can understand the existence of the thresholds near the hysteresis ranges of $[Br^-]_0$ for the subcritical Hopf bifurcations and no excitability of the steady states near the bifurcation points for the supercritical Hopf bifurcations. The thresholds in this system presumably depend on the values of the external parameters. Noszticzius et al. found that the BZ reaction (substrate: malonic acid) is excitable in its induction period and the threshold of excitability is decreasing gradually to zero during the period.[25] Therefore, a further study of excitation in the bromate-bromide-cerium(III) system may be very interesting.

A phase portrait explaining the behavior of this system depicted in Figs. 6a and 6b is shown in Fig. 7c; there is an unstable limit cycle around the stable focus of SSII, which corresponds to a separatrix, and another separatrix separates partially one basin in phase space. Figure 6b shows the excitation of the system in a bistable state. There is also a similar excitation in region e of Fig. 1. In the excitations, the separatrixes separating partially basins may correspond to sharp thresholds. When $[BrO_3^-]_0$=0.076 M and $[Br^-]_0$=2.303×10^{-4} M, SSI and SSII of this system never exchange each other's position by a perturbation of the bromide concentration. Therefore, the phase portrait shown in Fig. 7d is presumed for the system under the reaction condition.

The complicated behaviors described above, caused by the nonlinearity of the system, are consistent with one part of those in the model of Boissonade and De Kepper.[9,11] In this study, no other behavior was examined.

As shown in Fig. 1, the bromate-bromide-cerium(III) system in a CSTR exhibits bistability and sustained oscillations. This behavior is based on the autocatalytic formation of $HBrO_2$ due to a combination of Reactions 5 and 6. In order to understand the nonlinear property of the system in detail, we examined the dynamical behavior of a five-variable model composed of Reactions 1—4 and 7:

$$BrO_3^- + HBrO_2 + 2Ce(III) + 3H^+ \rightleftarrows 2HBrO_2 + 2Ce(IV) + H_2O. \quad (7)$$

We assumed that the forward step of Reaction 5 and the backward step of Reaction 6 are rate determining for the autocatalytic formation of $HBrO_2$ and for the reduction of cerium(IV) by $HBrO_2$, respectively. Such a condition can, perhaps, be realized when $[Ce(III)]_0$ is considerably high. Thus, the rates of Reaction 7 are yielded as

$$v_7 = k_7[H^+]_0[BrO_3^-]_0[HBrO_2] \quad (8)$$

and

$$v_{-7} = k_{-7}[Ce(IV)][HBrO_2], \quad (9)$$

where we assumed that $[BrO_3^-]$ is substantially equal to $[BrO_3^-]_0$, since the system studied here contains a large excess of bromate. The state of the model system depends on the four constraints, $[H^+]_0$, $[BrO_3^-]_0$, $[Br^-]_0$, and k_0. We reported previously that the four-variable model neglecting the backward step in Reaction 7 reproduced only bistability.[8] The five-variable model in this study reproduces both bistability and sustained oscillations, as described below.

The rate equations generated from the five-variable model are written as follows:

$$d[Br_2]/dt = k_1[H^+]_0[Br^-][HOBr] - (k_0 + k_{-1})[Br_2], \quad (10)$$

$$\begin{aligned} d[HBrO_2]/dt = {} & k_3[H^+]_0^2[BrO_3^-]_0[Br^-] \\ & - k_{-3}[HBrO_2][HOBr] - k_2[H^+]_0[Br^-][HBrO_2] \\ & - 2k_4[HBrO_2]^2 + k_7[H^+]_0[BrO_3^-]_0[HBrO_2] \\ & - (k_{-7}/2)[Ce(IV)][HBrO_2] - k_0[HBrO_2], \end{aligned} \quad (11)$$

$$\begin{aligned} d[HOBr]/dt = {} & k_3[H^+]_0^2[BrO_3^-]_0[Br^-] \\ & - k_{-3}[HBrO_2][HOBr] + k_{-1}[Br_2] \\ & - k_1[H^+]_0[HOBr][Br^-] + 2k_2[H^+]_0[Br^-][HBrO_2] \\ & + k_4[HBrO_2]^2 - k_0[HOBr], \end{aligned} \quad (12)$$

$$\begin{aligned} d[Br^-]/dt = {} & k_{-3}[HBrO_2][HOBr] - k_3[H^+]_0^2[BrO_3^-]_0[Br^-] \\ & + k_{-1}[Br_2] - k_1[H^+]_0[HOBr][Br^-] \\ & - k_2[H^+]_0[Br^-][HBrO_2] + k_0([Br^-]_0 - [Br^-]), \end{aligned} \quad (13)$$

and

$$\begin{aligned} d[Ce(IV)]/dt = {} & 2k_7[H^+]_0[BrO_3^-]_0[HBrO_2] \\ & - k_{-7}[Ce(IV)][HBrO_2] - k_0[Ce(IV)]. \end{aligned} \quad (14)$$

In this examination, we used $[H^+]_0$=0.75 M, k_0=0.005 s^{-1}, k_7=25 M^{-2}s^{-1} and k_{-7}=2×10^4 M^{-1}s^{-1}. When $[BrO_3^-]_0$=0.06 M, the model exhibits bistability in the $[Br^-]_0$ range of 8.16×10^{-5}—1.19×10^{-4} M. When $[BrO_3^-]_0$=0.25 M, it exhibits sustained oscillations in the $[Br^-]$ range of 6.22×10^{-4}—8.43×10^{-4} M (Fig. 8a (period: 260 s)). In order to reduce the number of independent variables to two, we adopted a quasi-stationary state approximation. We assumed the following combination of stationary states.

$$d[Br_2]/dt = 0, \; d[HOBr]/dt = 0, \text{ and } d[Br^-]/dt = 0. \quad (15)$$

We should note that the sustained oscillations can not be reproduced under the assumption that $d[Ce(IV)]/dt = 0$. We obtained the $HBrO_2$ and Ce(IV) nullclines by using Eqs. 10—15. Figure 8b shows the nullclines in the ($[HBrO_2]$, $[Ce(IV)]$, $[Br^-]$) space when $[BrO_3^-]_0$

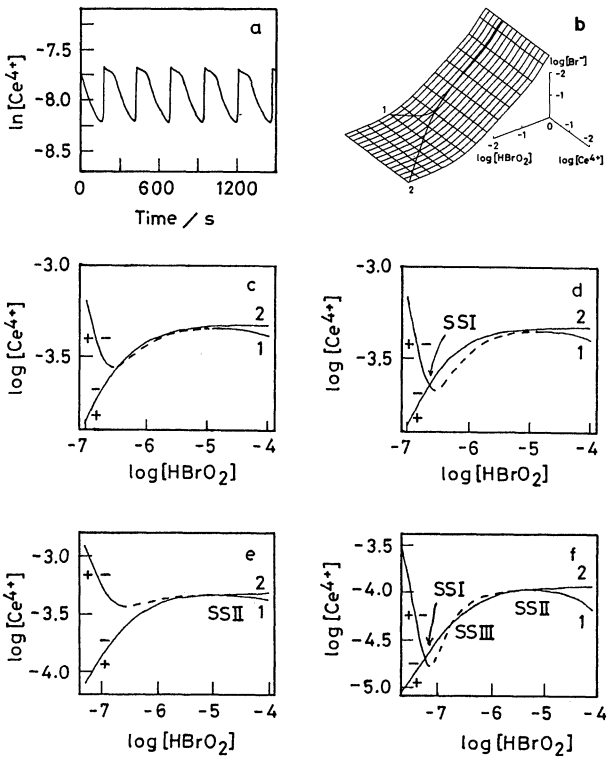

Fig. 8. Oscillations and $HBrO_2$ and Ce(IV) nullclines of the five-variable model.
$[H^+]_0$=0.75 M, k_0=0.005 s^{-1}, k_7=25 $M^{-2}s^{-1}$, and k_{-7}=2×10⁴ $M^{-1}s^{-1}$.
a: oscillations when $[BrO_3^-]_0$=0.25 M and $[Br^-]_0$=7.5×10⁻⁴ M. b: nullclines in the ($[HBrO_2]$, [Ce(IV)], $[Br^-]$) space when $[BrO_3^-]_0$=0.25 M and $[Br^-]_0$=7.5×10⁻⁴ M. c: $[BrO_3^-]_0$=0.25 M and $[Br^-]_0$=7.5×10⁻⁴ M, d: $[BrO_3^-]_0$=0.25 M and $[Br^-]_0$=10⁻³ M, e: $[BrO_3^-]_0$=0.25 M and $[Br^-]_0$=4×10⁻⁴ M, f: $[BrO_3^-]_0$=0.06 M and $[Br^-]_0$=9×10⁻⁵ M.
1: $d[HBrO_2]/dt$=0, 2: d[Ce(IV)]/dt=0. +: $d[HBrO_2]/dt$>0 or d[Ce(IV)]/dt>0, −: $d[HBrO_2]/dt$<0, or d[Ce(IV)]/dt<0.

=0.25 M and $[Br^-]_0$=7.5×10⁻⁴ M. The figure suggests that the model has no folded slow manifold, as expected from Eqs. 12, 13, and 15. Figures 8c—8f show the nullclines projected on the $[HBrO_2]$-[Ce(IV)] plane when $[BrO_3^-]_0$=0.06 and 0.25 M. Because all of the $HBrO_2$ nullclines in the figures have S-shapes, there are unstable regions in the nullclines (dashed lines in Figs. 8c—8f). The intersections of the $HBrO_2$ and Ce(IV) nullclines correspond to the steady states in the model system. In Fig. 8c since the intersection exists in the unstable region the state of the model system never settles down into the steady state, though stable steady states (SSI and SSII) can be seen in Figs. 8d and 8e. There are three intersections (one unstable and two stable steady states) in Fig. 8f.[26] That is, the model system is bistable under the reaction condition. The backward step in Reaction 7 indicates a decay of $HBrO_2$ formed autocatalytically. Such a decay process may be necessary for the occurrence of sustained oscillations in the bromate-bromide-cerium(III) system, which is far simpler than a BZ reaction.

References

1) W. Geiseler and H. H. Föllner, *Biophys. Chem.*, **6**, 107 (1977).
2) W. Geiseler and K. Bar-Eli, *J. Phys. Chem.*, **85**, 908 (1981).
3) W. Geiseler, *Ber. Bunsenges. Phys. Chem.*, **86**, 721 (1982).
4) K. Bar-Eli and W. Geiseler, *J. Phys. Chem.*, **87**, 3769 (1983).
5) R. J. Field, E. Körös, and R. M. Noyes, *J. Am. Chem. Soc.*, **94**, 8649 (1972).
6) K. Bar-Eli and J. Ronkin, *J. Phys. Chem.*, **88**, 2844 (1984).
7) R. J. Field and H.-D. Försterling, *J. Phys. Chem.*, **90**, 5400 (1986).
8) Y. Sasaki, *Bull. Chem. Soc. Jpn.*, **61**, 4071 (1988).
9) J. Boissonade and P. De Kepper, *J. Phys. Chem.*, **84**, 501 (1980).
10) P. De Kepper and J. Boissonade, "Oscillations and Traveling Waves in Chemical Systems," ed by R. J. Field and M. Burger, Wiley-Interscience, New York (1985), p. 223.
11) J. Guckenheimer, *Physica D*, **20**, 1 (1986).
12) C. W. Gear, "Numerical Initial Value Problems in Ordinary Differential Equations," Prentice-Hall, Englewood Cliffs, N. J. (1971).
13) The state of the system is oscillatory in region d and monostable (SSI or SSII) in region e.
14) E. Kumpinsky and I. R. Epstein, *J. Phys. Chem.*, **89**, 688 (1985).
15) G. Iooss and D. D. Joseph, "Elementary Stability and Bifurcation Theory," Springer-Verlag, New York (1980).
16) V. Gáspár, G. Bazsa, and M. T. Beck, *J. Phys. Chem.*, **89**, 5495 (1985).
17) In the calculation, we changed the initial value of $[Br^-]$ from its steady state value.
18) P. Ruoff, *Chem. Phys. Lett.*, **90**, 76 (1982).
19) By calculating in the same manner as described above, we can obtain the threshold of the subcritical Hopf bifurcation in regard to the bromide concentration when the system exists in a steady state (SSI or SSII) in the hysteresis regions in Fig. 3. Such a perturbation that the bromide concentration exceeds the threshold of the subcritical Hopf bifurcation induces the sustained oscillations of the system.
20) Z. Noszticzius, P. Stirling, and M. Wittmann, *J. Phys. Chem.*, **89**, 4914 (1985).
21) V. Gáspár and P. Galambosi, *J. Phys. Chem.*, **90**, 2222 (1986).
22) J. J. Tyson, *J. Chem. Phys.*, **66**, 905 (1977).
23) K. Bar-Eli and R. M. Noyes, *J. Chem. Phys.*, **86**, 1927 (1987).
24) The model of Boissonade and De Kepper presents a similar behavior more clearly to us.
25) Z. Noszticzius, M. Wittmann, and P. Stirling, *J. Chem. Phys.*, **86**, 1922 (1987).
26) The SSII-intersections in Figs. 8e and 8f exist in the unstable regions near the turning points of the $HBrO_2$ nullclines. These intersections represent stable foci because the model system has no slow manifold.